Eur Biophys J (2012) 41:851–861
DOI 10.1007/s00249-012-0843-3

REVIEW

EBSA
Biophysics in Europe

X-ray lithography and small-angle X-ray scattering: a combination of techniques merging biology and materials science

B. Marmiroli · H. Amenitsch

Received: 9 April 2012 / Revised: 30 June 2012 / Accepted: 10 July 2012 / Published online: 2 August 2012

Abstract The advent of micro/nanotechnology has blurred the border between biology and materials science. Miniaturization of chemical and biological assays, performed by use of micro/nanofluidics, requires both careful selection of the methods of fabrication and the development of materials designed for specific applications. This, in turn, increases the need for interdisciplinary combination of suitable microfabrication and characterisation techniques. In this review, the advantages of combining X-ray lithography, as fabrication technique, with small-angle X-ray scattering measurements will be discussed. X-ray lithography enables the limitations of small-angle X-ray scattering, specifically time resolution and sample environment, to be overcome. Small-angle X-ray scattering, on the other hand, enables investigation and, consequently, adjustment of the nanostructural morphology of microstructures and materials fabricated by X-ray lithography. Moreover, the effect of X-ray irradiation on novel materials can be determined by use of small-angle X-ray scattering. The combination of top-down and bottom-up methods to develop new functional materials and structures with potential in biology will be reported.

Keywords Small-angle scattering · Deep X-ray lithography · Bottom-up top-down manufacturing · Radiation-assisted material synthesis and processing

Special Issue: Scattering techniques in biology—Marking the contributions to the field by Peter Laggner, on the occasion of his 68th birthday.

B. Marmiroli · H. Amenitsch (✉)
Institute of Biophysics and Nanosystems Research, Austrian Academy of Sciences, Schmiedlstr. 6, 8042 Graz, Austria
e-mail: amenitsch@elettra.trieste.it

Introduction

"Interdisciplinarity" is an important aspect of modern science (Choi and Pak 2006). By adopting this principle, the advent of micro-nanotechnology has increasingly merged previously separate fields, for example biology and materials science (Ozin and Cademartiri 2009). Microtechnology and, in particular, micro/nanofluidics are the basis of miniaturization of chemical biological assays, because they enable reduction of the amount of sample by as much as a factor of one million, achievement of excellent spatial and temporal resolution, facilitation of parallel analysis, increased throughput, and reduced cost. The principles of operation of these devices, based on micro/nanofluid physics, cannot be achieved at the macroscale. To some extent, micro/nanotechnology is affecting biology and chemistry in the same way as microprocessors affected electronics. Today, microcomponents are fabricated from different materials (plastics, elastomers, metals, ceramics, gels, silicon, glass, paper). The choice of fabrication technology and material is important because it leads to micro/nanostructures with different features (chemical and biological compatibility, thermal stability, gas exchange, hydrophobicity/philicity). Moreover, for many (bio)applications, a combination of different materials and surface chemistry may be needed (Vyawahare et al. 2010).

Given these premises, interdisciplinarity becomes fundamental also in the combination of microfabrication and characterization techniques, both of which are used in the construction of new devices and in the development of novel materials for applications in chemistry and biology.

In this review, we emphasise the advantages of combining the techniques deep X-ray lithography (DXRL) for microfabrication and small-angle X-ray scattering (SAXS) for structure determination. DXRL enables SAXS to

overcome time resolution and sample environment limitations whereas SAXS enables examination of the nanostructural morphology of the microstructures fabricated by DXRL, for example for adjustment of the morphology for specific applications, for example (bio)nanosensors, or determining the effect of irradiation on novel materials.

Examples of both will be presented. First, microdevices fabricated for time-resolved experiments on biological and chemical reactions or for study of the effect of confinement on crystal growth will be discussed. Second, the combination of bottom-up and top-down approaches to the development of new functionalized materials and structures with important applications in biotechnology, and for which characterization with SAXS/wide-angle X-ray diffraction (WAXD) is fundamental, will be described.

The techniques

In this section short descriptions of XRL and SAXS are given.

XRL is a manufacturing process in which a material (called *resist*), the dissolution rate of which in a liquid solvent (called *developer*) changes under high-energy irradiation, is exposed to synchrotron radiation through an X-ray mask. The mask usually consists of a pattern of a strongly X-ray-absorbing material (typically gold) supported by thin membranes made of silicon nitride, titanium, graphite, or polymers that for transparency reasons are just few micrometers thick and that extend over areas of several square centimetres. Where the beam is not stopped by the adsorbing material, it is transmitted by the membrane and exposes the resist deposited on the target substrate. The resist is defined as *positive* if the exposed part dissolves in the developer and *negative* if it crosslinks upon exposure and the unexposed parts dissolve in the developer. In both cases, after development, the resist has the same geometrical features as the original pattern of the mask (Fig. 1). If the energy range of the X-rays used for the process is high (peak of the energy range distribution approx. 8 keV) we talk about DXRL. DXRL can be regarded as the best lithographic technique in respect of depth of penetration of thick resists and high aspect ratio patterns. Moreover, the structures obtained have vertical sidewalls with optical surface quality (Tormen et al. 2011). Since its introduction (Becker et al. 1986), DXRL has been used to fabricate microcomponents directly from plastics (mainly poly(methyl methacrylate), PMMA, and SU-8 epoxy resin (del Campo and Greiner 2007)) or from metal and ceramics by use of the so-called *LIGA* (Litografie, Galvanoformung, Abformung = lithography, electrodeposition, moulding) process. In LIGA, the resist is deposited on a conducting substrate, and the structure obtained after irradiation and development is used as a template in an electroforming process in which metal is deposited on to the electrically conductive substrate in the spaces between the resist structures.

The metallic object obtained after removal of the resist can then be used as an electrode in a subsequent electro discharge machining process, or as a mould for hot embossing or injection moulding or even ceramic sintering. This technique enables production of many components in, for example, micromechanics, microoptics, microfluidics, and microelectronics (Perennes et al. 2006; Romanato et al. 2006; del Campo and Arzt 2008; del Campo and Greiner 2007; Saile et al. 2009).

More recently, a new field of application of XRL has been investigated. It consists in irradiation of novel materials and in the study of the related structural changes (Falcaro and Innocenzi 2011).

SAXS is used as a standard method for characterization of structure at the nanoscale, i.e. between 1 and 100 nm (Feigin and Svergun 1987). Although this structural range can be accessed with other techniques, for example electron microscopy or solution NMR, SAXS is much more versatile in respect of sample preparation and environment (solid, liquid, or gas). Moreover, the technique has excellent in-situ capabilities. One disadvantage is the spatial resolution of the technique, which is intrinsically limited by the rotational and ensemble averaging of the measured structures which occurs. However, detailed information can be obtained, averaged over the whole volume exposed. The principal arrangement is shown schematically in Fig. 1b, inset (1), in which the sample/scattering geometry is given. X-rays scattered by the sample are detected by a two-dimensional detector. Depending on the inner structure of the sample an ordered, partly ordered, or random scattering pattern can be obtained (Amenitsch and Marmiroli 2011). Usually, SAXS is conducted in transmission geometry. If the sample is composed of a film deposited on a substrate, it is better to use grazing-incidence (GISAXS) rather than transmission geometry for the measurement, as shown in Fig. 1b, inset (2). The sample is aligned near to or at the substrate critical angle of total reflection. The incident beam is therefore reflected and refracted primarily by the substrate, and the refracted beam penetrates the film. The film gives rise to small-angle scattering around the refracted beam. Although there are SAXS contributions from the incident, reflected, and refracted beams, GISAXS patterns show that the contribution from the refracted beam is dominant (Levine et al. 1989).

Lithography and SAXS: devices for biology and materials science

As already stated, micro and nano fabrication techniques enable the construction of devices and systems on the basis

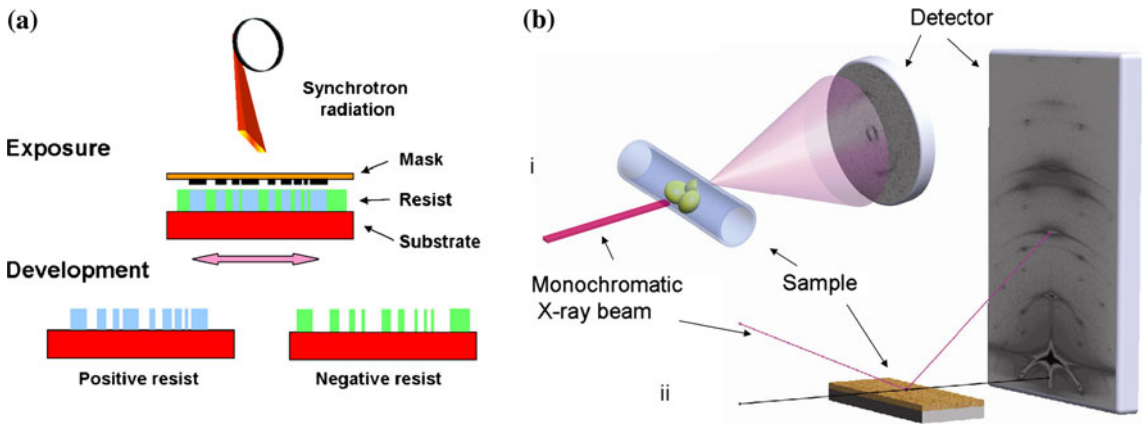

Fig. 1 **a** Schematic diagram of the X-ray lithography process. It is based on exposure to the white synchrotron beam and development of a material which is sensitive to X-rays. The positive resist dissolves in the developer after irradiation, resulting in the absorber pattern of the mask. The negative resist undergoes crosslinking as a result of irradiation, leading to holes corresponding to the absorber pattern of the mask. **b** Typical small-angle X-ray scattering set-up. A monochromatic X-ray beam is directed at a sample and scattered radiation is collected by a detector: (*i*) scattering from partially ordered samples; (*ii*) grazing incidence small-angle X-ray scattering from a solid supported film

of physical principles different from those used on the macroscale, enabling new concepts in instruments or experiments.

In particular, microfluidics (microchannels, micromixers, microwells) precisely manipulate and control biological and chemical entities. Small amounts of sample are handled. This is relevant, especially for biological samples which are usually expensive, and available in small quantities only. With regard to micromixers, because of the small dimensions of the channels, mixing occurs faster and with more control; time-resolved measurements can therefore be enhanced. Moreover, the effect of confinement on reactions can be investigated.

As a result of the strong synergy between state of the art microtechnology and advanced measurement and manipulation techniques, it is possible to investigate new topics (e.g. parallel combinatorial chemistry, mass screening, single-particle analysis). In the next two sections examples of the creation of microdevices to gain insight into chemical and biological reactions are reported. In both, DXRL is used for fabrication and SAXS as measurement technique.

Micromixer for studying fast chemical and biological reactions

Design and engineering of micron and submicron functional colloidal particles have attracted much attention in the last decade because of their biotechnological and nanotechnological significance and their potential for exploitation in biology and medicine (Sukhorukov et al. 2004). Important features of nanoparticles, for example lattice type, dimension, size distribution, and effect of additives on the particles, are already defined in the early stages of the reaction. For this reason, numerous studies have been conducted on the initial stages of nanoparticles formation. Moreover, short time-scales are particularly interesting for gaining insight into fast biological reactions, for example conformational changes of proteins. Examining the sequence of structural changes associated with the unfolding of a protein is challenging, because important structural events occur on the microsecond time scale, which cannot be accessed by conventional kinetic techniques (Roder et al. 2006). Use of micromixers results in improved time resolution, and exploitation of microfluidics in combination with SAXS has enabled time-resolved measurements with a resolution of a few tenths of microseconds (Otten et al. 2005; Panine et al. 2006; Amenitsch and Marmiroli 2011). In this context, we have designed, fabricated, and tested a microfluidic mixer, with very high time resolution, designed for studies of fast chemical reactions (Marmiroli et al. 2009). The mixer is based on hydrodynamic focussing and results in laminar mixing. Its geometry and dimensions are stringent (channels 10 μm wide and >60 μm deep with features of 1 μm); this required a fabrication process based on DXRL performed at the DXRL beamline at Elettra (Perennes et al. 2002). Mixing is completed inside the device before the nozzle, and the time evolution of the reaction is separated spatially in the steady state flow along the liquid jet leaving the device (Fig. 2a). Even if the device has been optimized for synchrotron SAXS measurements (Marmiroli et al. 2010), choice of a free jet as observation region overcomes the problem of selection of the material for the microfluidic chamber. This enables use of the same device with different investigation techniques (e.g. UV and Raman spectroscopy). The device usually works with a jet speed of

13 m/s, and a mixing time of 45 μs. Experiments conducted at the Austrian SAXS beamline at Elettra (Amenitsch et al. 1997), have shown that formation of $CaCO_3$ nanoparticles can be detected as soon as 75 μs after mixing, and the course of the reaction was followed, as shown by the intensity curves in Fig. 2b and by the invariant of Fig. 2c.

In biological reactions, the maximum pressure inside the device is less than the denaturation limit for proteins. The shear rate is not sufficient to destabilize a typical small protein of ~100 amino acids in water, but it could affect larger proteins or when using viscous solvents. Therefore, the possibility of using the device with biological reagents must be evaluated for each specific case.

Patterned supports to position and functionalize metal–organic framework crystals

Metal–organic frameworks (MOFs) are a new emerging class of hybrid porous materials with customized chemical composition. Because of their surface area of thousands of square metres per gram, controlled size, and distribution of pores, MOFs are promising candidates for application in filtration, sensing, and catalysis. However, for fabrication of MOF-based devices, MOF growth in selected locations would be required, and conventional synthetic routes are not suitable, because there is still a lack of knowledge on controlling MOF growth locations (Davis 2002).

Falcaro et al. (2011) investigated the possibility of using ceramic micro-particles, named "Desert Rose Microparticles" (DRMs), as seeds for MOFs nucleation. When surfactant Pluronic F127 is added to a traditional MOF-5 precursor solution it coordinates the Zn^{2+} ions and simultaneously provides an abundant source of phosphate. These factors enable the rapid formation of inorganic polyhydrate zinc phosphate nano-flaked microparticles: DRMs. Because DRM formation precedes the growth of MOF-5, DRMs can effectively act as heterogeneous nucleation seeds for the framework crystals.

During the first 3 h of reaction, only DRMs form. Heterogeneous nucleation of MOF-5 then occurs on the nanoflakes of the DRMs, leading to cubic crystallites. Growing for a longer time enables single crystals or multifaceted MOF-5 crystallites, that can reach the size of 100 μm, to be obtained. During a single-pot synthesis, DRMs can be isolated before nucleation of MOF-5, and re-dispersed into a variety of solvents as exogenous nucleation seeds. When incubated in a fresh *N*,*N*-diethylformamide (DEF)-based MOF-5 growth medium, a significant improvement in crystal quality can be achieved. This was determined by analysis of the X-ray diffraction pattern of the synthesized crystals (as can be seen in Fig. 3a).

Use of the nucleating agents more than doubles the crystal growth rate compared with control samples. Moreover, the seeded nucleation mechanism for growth of MOF-5 can be adapted directly to solid substrates. To

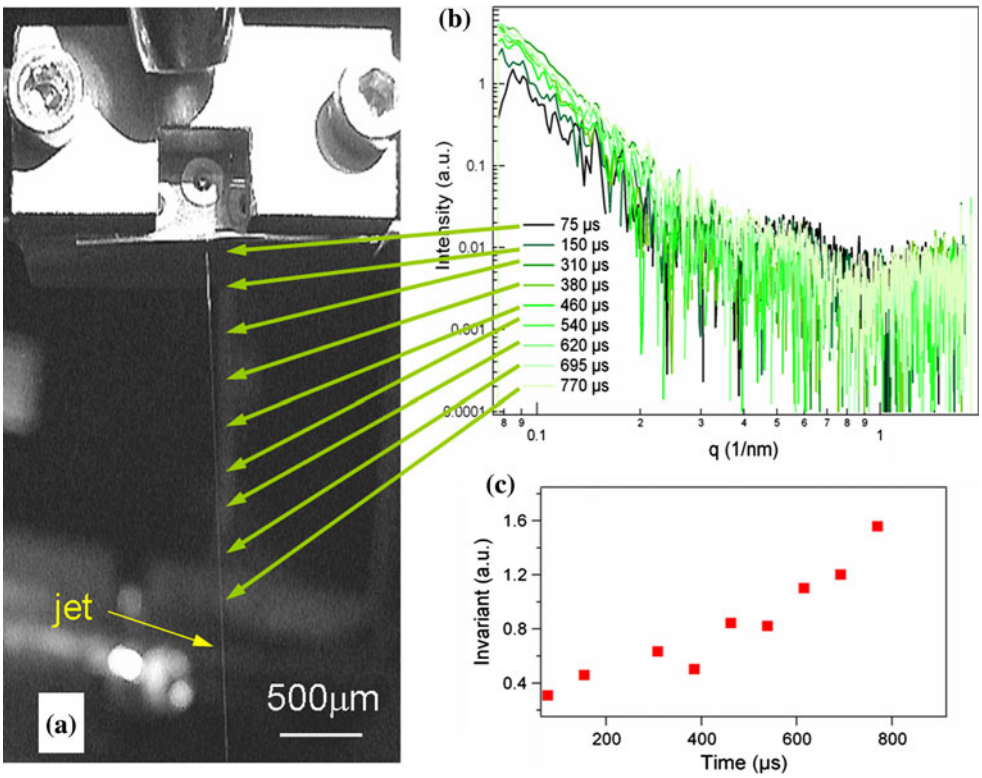

Fig. 2 **a** Micromixer fabricated by deep X-ray lithography, mounted on a stainless-steel sample holder. The micro free liquid jet in air leaves the mixer with a speed of 13 m/s. **b** Scattering curves of $CaCO_3$ formation in the time range 75–700 μs after the beginning of the mixing. **c** Invariant versus time. The increase of the invariant is because of the increment of the volume fraction of the particles, demonstrating evolution of the reaction (Marmiroli et al. 2009)

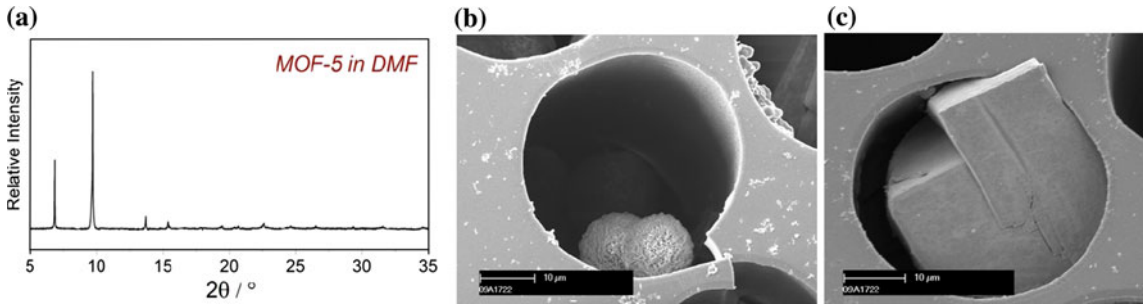

Fig. 3 **a** Measured diffraction patterns for MOF grown in different solvents (DEF and DMS) compared with a simulated pattern for ideal, defect-free MOF-5 crystals. These patterns showed that crystals grown in DMF as solvent had a higher defect concentration than those grown in DEF. **b** DRMs located in a hole of an array of wells fabricated by DXRL (*scale bar* is 10 μm). **c** MOF-5 crystal growing from DRM (*scale bar*, 10 μm) (Falcaro et al. 2011). Figures are adapted with permission

demonstrate this, a 100-μm layer of SU-8 resist on a silicon substrate was patterned by use of DXRL at the storage ring Elettra, to obtain an array of microwells (30–50 μm diameter). A few DRMs were then deposited in every well (Fig. 3b). Immersion of the array into an MOF-5 growth solution caused framework crystals to nucleate inside the wells (Fig. 3c). The crystallite sizes were first confined in the well; then, after growing beyond the top of the wells, they grew in all directions. The final system resulted in the merging of MOF crystals to form an interpenetrated crystalline structure that could be detached from the silicon wafer to form a free-standing support made of SU8 with circular holes containing MOFs. This demonstrated the capability to achieve controlled growth of MOF-5 crystals in a specific location, leading to MOF-based device fabrication.

SAXS and lithography: SAXS as a tool for investigation of radiation assisted-material synthesis and processing with DXRL

The development of nanomaterials is fundamental to the creation of devices with improved performance, for example in the field of drug delivery and biomedical diagnostics. In this context, the integration of nano and micro-fabrication techniques with bottom-up and top-down processing of materials is an important objective. Self-assembled mesoporous thin films are an example of materials synthesized with a bottom-up technique. Their integration into functional devices requires top-down processing (Brinker and Dunphy 2006). Brinker et al. have used different lithographic techniques to pattern mesoporous films (Doshi et al. 2000; Fan et al. 2000). These were based either on mesophase change or on mesostructure disruption occurring upon irradiation with UV light. The possibility of using electron beam lithography has also been investigated (Wu et al. 2004; Hozumi and Cheng 2011; Hozumi and Kimura 2008). Dip-pen nanolithography, ink-jet printing using a "self-assembling ink" (Lu et al. 2001), and selective de-wetting have been used to obtain patterned mesoporous arrays and microfluidic devices. A comprehensive review of conventional patterning techniques of mesostructured films has been written by Innocenzi et al. (2008). However, the need for functional integrated components requires techniques that enable high aspect-ratio, patterning thick layers, high resolution, and complex shapes to be achieved. For this reasons, DXRL is a very promising candidate for top-down patterning. Liu et al. (2003) were the first to pattern a sol–gel film with DXRL, but after their first experiment, they did not proceed to investigation of the effect of irradiation.

Some interesting applications of patterned organic–inorganic hybrid materials are in the field of optics and photonics. In fact, the versatility of sol–gel processing leads to a wide range of possibilities in the design of customized materials in terms of structure, functionality, and properties (Lebeau and Innocenzi 2011).

Mesoporous materials are well suited to sensing applications (Melde and Johnson 2010), for example for biological or electrochemical analysis (Walcarius and Kuhn 2008; Walcarius 2008). This is mainly because their surface area may exceed 1,000 m^2/g, and because of rapid diffusion of analytes through a porous structure. The ability to manipulate the structure and composition of these materials at different scales (from molecular to macromolecular states and/or from micro to meso and/or macroporous levels) will lead to the creation of chemical and biochemical sensing devices with improved selectivity and sensitivity (Walcarius and Collinson 2009), enabling also the mimicking of nature (Martinez-Manez et al. 2011a, b).

Mesoporous silica and organically-modified silica-based materials can also be used as filters to remove inorganic and organic pollutants from aqueous solutions (Walcarius and Mercier 2010).

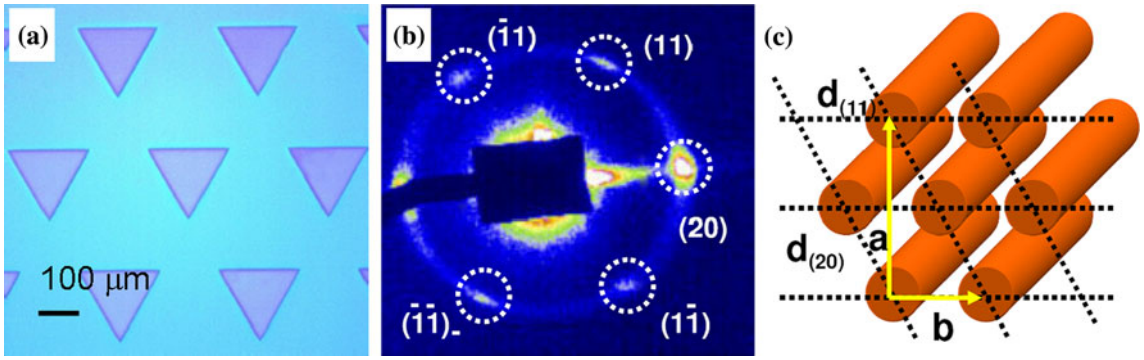

Fig. 4 **a** Optical microscopy images of a patterned mesostructured silica film revealing the different refractive indices of the exposed and the unexposed areas (**b**) GISAXS pattern of the cylindrical mesopores which are disposed according to a (**c**) two-dimensional hexagonal cross section with a p6 m symmetry group (Falcaro et al. 2008). Figures adapted with permission

In the following sections we report examples in which the bottom-up approach has been combined with the top-down DXRL process for patterning of complex materials and fabrication of functional devices. In all these examples SAXS has been used as investigation technique to check the quality of the process and to determine structural changes resulting from irradiation.

Patterning of thin films

Falcaro et al. (2008) have used DXRL to induce silica polycondensation. The unexposed areas of the film can be selectively etched, because of the lower degree of cross-linking of the inorganic network, and therefore act as a negative resist. An important advantage of DXRL is the possibility of simultaneously removing the surfactant and inducing condensation of the silica network. The patterned films (Fig. 4a) were examined by GISAXS (Fig. 4b, c) and transmission electron microscopy (TEM) to detect structural variation in the films' mesophases as a result of X-ray exposure. Moreover, Fourier-transform infrared imaging was used to characterize the induced chemical changes. After fabrication of mesoporous pillars by DXRL, they then used a dip-pen technique, using the tip of an atomic-force microscope (AFM), to selectively functionalize single pillars. A rhodamine 6G solution was used as ink to enable observation of the controlled writing by confocal fluorescence microscopy. Hierarchically-structured materials with organization at many length scales have been obtained: porosity (2–10 nm), film thickness (50–500 nm), and pattern size (1–150 µm). The ordered mesopores are an ideal host for functional organic molecules or nanoparticles (Innocenzi et al. 2004) and the patterns, from nano to micro scale, enable the design of devices for different types of advanced application (Scott et al. 2001), for example in DNA nanoarrays or lab-on-a-chip devices.

Falcaro et al. (2009) have also fabricated a hierarchical hybrid organic–inorganic thin film with pores in the meso and macro range and a very low refractive index. The first order of porosity was obtained by use of a self-assembly process using organic block copolymers as templates for mesopores. The mesophase was investigated in situ with GISAXS to identify its organization. Fluorinated organic nanoparticles were added to the precursor solution to template the second level of porosity. Introduction of the nanoparticles did not affect the organization of the mesophase, and, after deposition of the film, the nanoparticles were randomly dispersed in the matrix. After post-synthesis calcination at 350 °C hierarchical porous thin films with a bimodal distribution are obtained. Such films have a refractive index lower than that measured for monomodal mesoporous films. Films have also been patterned by use of DXRL and subsequently developed to obtain arrays of dots with bimodal hierarchical pore distribution.

These two examples reveal that DXRL of as-deposited sol–gel or mesoporous films, and subsequent chemical etching of the unexposed part of the film, is a direct method for obtaining complex structures made of dense and porous oxides and hybrid materials. Later, Costacurta et al. (2010) extended this method to samples prepared differently—by use of radio frequency plasma-enhanced chemical vapour deposition (PECVD), a typical technique for production of films. They used DXRL to investigate the effect of X-rays on as-deposited PECVD hybrid organic–inorganic films. This preliminary study has enabled optimization of the process to obtain well defined and high-quality patterned structures.

Costacurta et al. (2011) have also fabricated microstructures of ordered mesoporous silica, by use of a different technique but still based on DXRL. In fact, they first patterned hydrophilic/hydrophobic surfaces on perfluoroalkyl-functionalized surfaces by use of DXRL, thus obtaining a spatially defined wettability circuit (that could

also be exploited in microfluidic devices). Then, by a selective dewetting of the coating sol on the hydrophilic/hydrophobic fluorinated substrate, mesoporous silica structures were obtained. This technique is preferable to direct patterning when the mesoporous film contains organic functional groups which could be damaged by exposure to X-rays.

Faustini et al. (2011) used DXRL to pattern nanoperforated titania membranes obtained from a sol–gel solution by using block copolymer micelles as templating agent. They performed structural and electrochemical characterization to demonstrate that the final materials are micrometric features of a sub-10 nm thick perforated titania membrane that guarantees accessibility to the substrate. GISAXS measurements by use of laboratory equipment enabled determination of the structure of the films and the period of the array of nanoperforations. They applied this technique to a conductive platinum-coated silicon surface and achieved micrometric features of nanoelectrode arrays.

Patterning of titanosilicate mesoporous pillared planar nanochannels

Micro and nanofluidics are important for biology, because of the possibility of manipulating small amounts of samples. Nanofluidics, in particular, can be substantially affected by synthesis and modification of nanomaterials. In this context, an advantageous strategy is the synthesis and integration of nano-units of materials to create complex structures at low cost. This can be achieved by combining top-down and bottom-up techniques. Returning to fluidics, the kinetics of fluid diffusion within the channels are mainly dependent on the channels' dimensions, morphology, and surface chemistry. The presence of nanopillars, and their additional functionalized interfaces, inside selected areas of the channels, would help further adjustment of device properties.

Faustini et al. (2010) have fabricated large areas of mesofluidic pillared planar nanochannels (PPNs) made of vertical nanopillars with controlled dimensions, porosity, and chemical composition supporting a continuous roof of the same material. An example of a TiO_2 PPN is shown in Fig. 5a. PPNs have been obtained by combining self-assembly of block copolymer, nanostructured sol–gel coatings, and highly controlled liquid deposition processing. The structure has two types of porosity—an open interpillar porosity with adjustable dimensions between 20 and 200 nm and the porosity inside the pillars and roof, composed of pores less than 10 nm in diameter. Moreover, they can be patterned by use of DXRL and subsequent development, as demonstrated by the group (Fig. 5b). PPNs have been characterized by GISAXS to assess pillar ordering and mesostructure, as shown in Fig. 5c, d. The group also demonstrated that fluids can easily diffuse into the nanochannels of PPNs, in accordance with the predictions of the laws of nanofluidics.

PPNs are promising structures for preparation of nanofluidic channels to handle, concentrate, isolate, react, condition, and analyse dissolved species (i.e. ions, proteins,

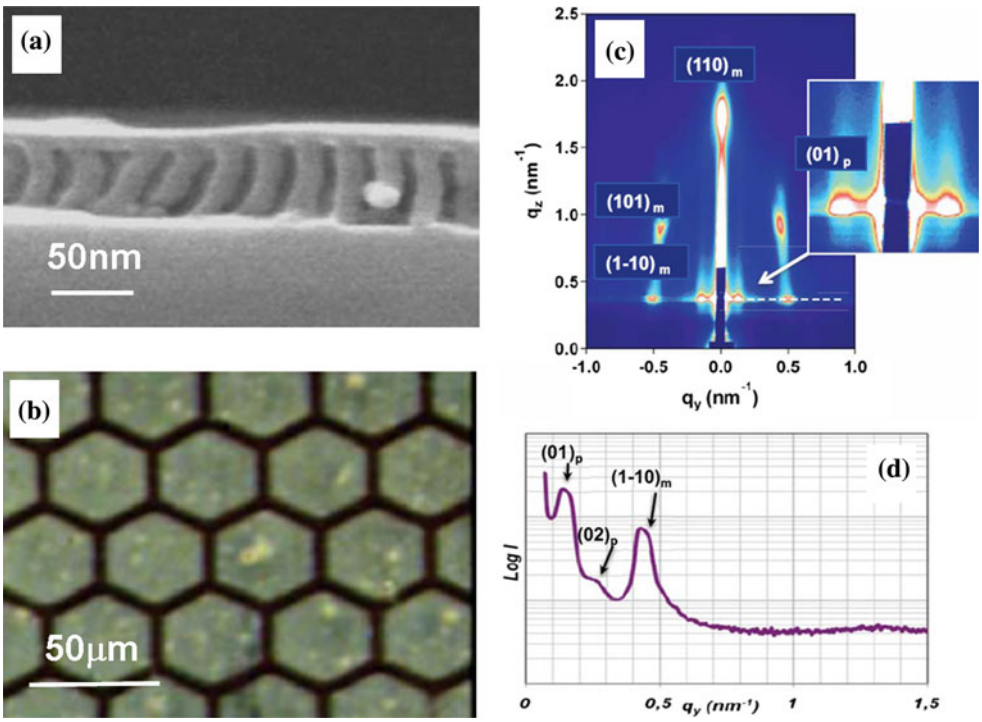

Fig. 5 **a** TEM image of a pure TiO_2 PPN (**b**) Optical image of PPN after X-ray lithography and development. The continuous part corresponds to the exposed areas where materials have been stabilized. The hexagonal pattern has dimensions of 40 μm. **c** GISAXS pattern of an F127-templated 10 % SiO_2–90 % TiO_2 PPN, with the typical Bragg points of a Im3m mesostructure at higher q value and the diffraction rods associated with the pillar periodicity at lower q values. **d** Plot of the diffused intensity (log I) versus the wave vector in the y direction of the reciprocal space, showing both lateral periodicities (Faustini et al. 2010). Figures adapted with permission

DNA). In fact, because of their large area, they are more efficient than dense PPNs.

In-situ synthesis of nanoparticles

The surface plasmon resonance of gold and silver nanoparticles is an important phenomenon that has already been used in new analytical techniques. The plasmon resonance effect is caused by collective oscillation of the noble metal valence electrons resonantly excited by visible light; this causes a strong enhancement of the electromagnetic near-field in molecules that are in close proximity to the particles. Because of this effect, molecules adsorbed by these noble metal particles or that are at a distance smaller than 10 nm feel a field up to 100 times more intense than the direct excitation in a plasmon-free environment. Thus, Raman scattering of adjunct molecules and their luminescence can be greatly enhanced (Nie and Emory 1997). These phenomena are commonly known as surface-enhanced Raman scattering (SERS) or, more generally, metal-enhanced luminescence (MEL). However, MEL can be confused with "classical" luminescence energy transfer between the metal particle and the luminescent molecule. In a Forster resonance energy-transfer process, the donor chromophor absorbs the excitation light first and then transfers the energy by a non-radiative multipole coupling mechanism to the acceptor luminophor. For noble metal particles the correct assignment of the different enhancement mechanisms depends on particle size. To fully exploit this luminescence enhancement it is very important to be able to control the size and distribution of nanoparticles in the host matrix. The different methods of activation and control of the emission colours have great potential for realization of a variety of devices, for example glass fibre lasers, optical memory, or novel white-light sources (Eichelbaum and Rademann 2009).

Eichelbaum et al. have reported a novel method of generating high concentrations of nearly monodisperse gold nanoparticles in soda-lime silicate glasses by exposing samples to synchrotron light (Eichelbaum and Rademann 2009; Eichelbaum et al. 2005, 2008; Tatchev et al. 2011) at the DXRL beamline at the Berlin electron storage ring (BESSY II) (Loechel et al. 2007). Subsequent annealing at 550 °C induces the growth of larger particles. The effect of this process is shown by optical microscopy in Fig. 6a and by means of a confocal fluorescence image of the same areas in Fig. 6b. With this method, nucleation is generated by irradiation, and growth by annealing. The two mechanisms are separated; thus cluster size and number density can be modified by changing annealing time or temperature. Synchrotron SAXS measurements revealed the dependence of annealing time on particle size distribution: the gold cluster radius increases with annealing (Fig. 5c, d). Tatchev et al. (2011) have also used ASAXS to observe in-situ formation of gold nanoparticles in soda lime silicate glass under constant X-ray irradiation, comparing it with

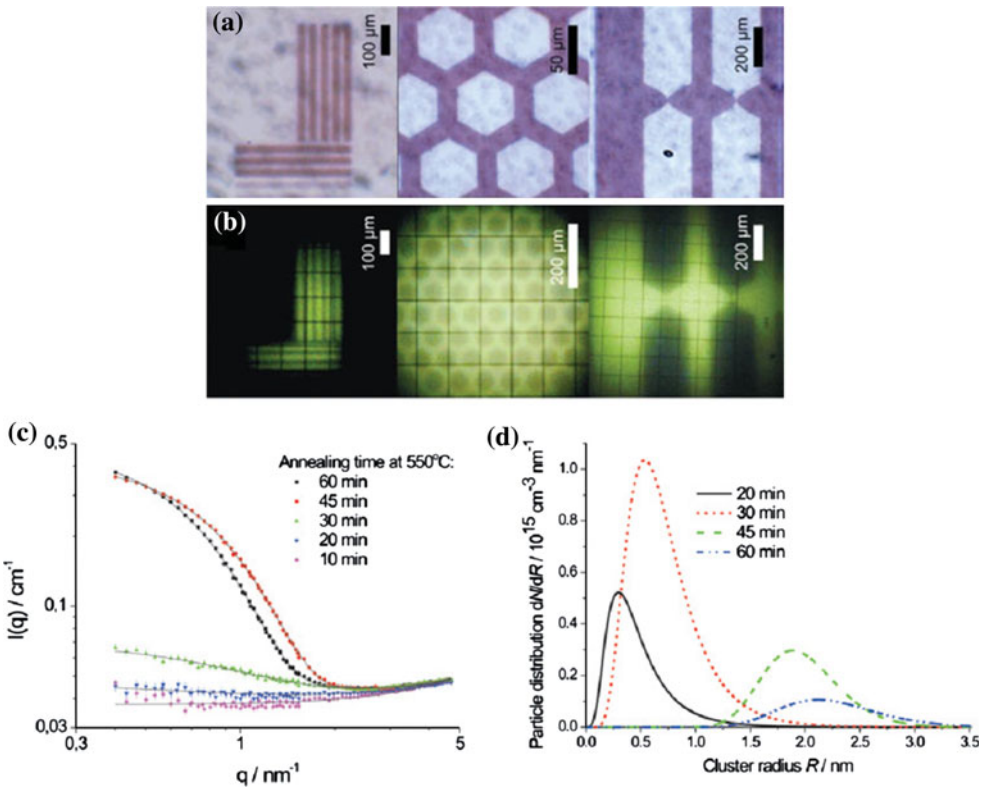

Fig. 6 **a** Optical microscope image of lithographically activated Au-doped glasses after annealing for 45 min at 550 °C. **b** Confocal luminescence microscope images of the same structures shown in **a**, but annealed for 5 min at 550 °C. **c** Scattering curves of gold glasses irradiated and annealed at 550 °C for different times. The *black lines* represent fits with spherical particles with log–normal size distribution. **d** SAXS particle size distributions for gold nanoparticles after irradiation and annealing at 550 °C for different times (Eichelbaum and Rademann 2009; Eichelbaum et al. 2008). Figures adapted with permission

ex-situ formation in pre-irradiated glasses. After excitation with a commercial UV LED, the gold and silver nanoparticles produced after irradiation and different annealing times and temperatures had different emission colours. Emission colours which can be adjusted are very promising for the development of bright light-emitting devices (Eichelbaum and Rademann 2009).

Malfatti et al. (2010) have extended this technology to obtain functional nanomaterials containing nanoparticles. They used DXRL to fabricate patterned microstructures of mesoporous materials containing gold nanoparticles in a single step. In fact, X-rays interact with the mesoporous matrix by removing the organic templates, by increasing the polycondensation of the organic–inorganic silica network, and by partially removing the methyl groups bonded in the hybrid matrix. They also promote nucleation of gold nanoparticles. After exposure, the mesoporous film containing the nanoparticles is developed to remove the unexposed part of the film. The final material, after patterning and chemical etching, was measured by GISAXS, which showed it contained gold nanoparticles of a few nanometres homogeneously dispersed in the porous matrix. Because DXRL uses high-energy X-rays, it can also penetrate thick films, enabling the fabrication of patterned structures with high aspect ratios. Moreover, the material mesostructure is not affected by exposure to X-rays and etching. Malfatti et al. (2011) have also fabricated mesoporous nanocomposite materials containing silver nanoparticles by using evaporation-induced self-assembly and DXRL. These combined processes result in a nanocomposite material which has a 2D hexagonal organized porosity and silver nanoparticles with a precise size distribution around 5 nm. They compared the Raman response in the exposed and unexposed areas, and showed that in the unexposed part the intrinsic sensitivity of Raman spectroscopy does not enable detection of the dye whereas the characteristic Raman spectrum of Rh6G could be detected in the exposed part where silver nanoparticles are grown by X-rays.

Metrology

SAXS can be used as a quality control technique for lithographically prepared microstructures with potential as bio-arrays or bio-diagnostics. The NIST (National Institute of Standards and Technology: http://www.nist.gov/index.html) has demonstrated the application of SAXS as a new measurement method for non-destructive characterization of size and shape at nanometric length scales. Current measurement methods, for example scanning electron microscopy, atomic-force microscopy, and optical scatterometry, face challenges in the characterization of dense, high-aspect-ratio nanoscale features because, in general, smaller structures are increasingly difficult to measure. In contrast, precise measurement of nanoscale structures by use of SAXS become easier with decreasing structural size. The focus is on delivering a technique performing routine measurement of pattern shape, critical dimensions, sidewall angle, width fluctuations, line edge roughness, and statistical deviations across large areas in dense high-aspect-ratio patterns (Wang et al. 2007; Zschech et al. 2011). Quality control is, in fact, fundamental for up-scaling of micro–nano technology to an industrial level.

Nazmov et al. (2011a, b) have fabricated parabolic crossed planar polymeric X-ray lenses which enable focussing in one and two directions; these could have applications in X-ray imaging and analysis. In fact, by using these lenses, spatial resolution down to 20 nm can theoretically be achieved. They fabricated the lenses by DXRL at the X-ray lithography beamlines LIGA-I, LIGA-II, or LIGA-III at ANKA synchrotron (Goettert et al. 2000) by using two kinds of polymer—negative and positive. They then investigated, by SAXS, the X-ray scattering level after a large number of microstructures with flat sidewalls (bi-prisms of the negative polymer with different sidewall inclination angles) and found that the scattering background is too low to affect sub-micron focussing.

Conclusion

As emphasised by Vyawahare et al. (2010), the possibility of using micro/nano technology for “digital biology” will enable us to handle biological assays at the single-molecule, single-cell, or single-organism level. The combination of microfabrication and investigation techniques therefore becomes fundamental to the development of a suitable sample environment. In this review we have presented the combination of DXRL and SAXS as example of the possibilities offered by interdisciplinarity to both chemistry and biology. DXRL has enabled the creation of microfluidic devices to handle chemical and biological assays to improve SAXS measurement and to investigate new effects, for example confinement. SAXS has been used to determine the nanostructural morphology of DXRL structures, to modify the fabrication process and/or the properties of novel irradiated materials, and obtain new improved (bio)micro-nanodevices.

Acknowledgments B. Sartori is acknowledged for the help with preparation of some of the figures. The authors particularly thank the small angle-scattering-group from the Austrian SAXS beamline, which contributed to parts of this work, namely: F. Cacho-Nerin, K. Jungnikl, I. Shyjumon, F. Schmid, D. Jozic, C. Morello, M. Rappolt, S. Bernstorff and, most notably, P. Laggner, who initiated and led the project of the Austrian SAXS beamline at the synchrotron ELETTRA, Trieste.

References

Amenitsch H, Marmiroli B (2011) Time-resolved structure investigation with small-angle X-ray scattering using scanning techniques. Rendiconti Lincei 22:S93–S107

Amenitsch H, Bernstorff S, Kriechbaum M, Lombardo D, Mio H, Rappolt M, Laggner P (1997) Performance and first results of the ELETTRA high-flux beamline for small-angle X-ray scattering. J Appl Crystallogr 30:872–876

Becker EW, Ehrfeld W, Hagmann P, Maner A, Muenchmeyer D (1986) Fabrication of microstructures with high aspect ratios and great structural heights by synchrotron radiation lithography, galvanoforming, and plastic moulding (LIGA process). Microelectron Eng 4:35–56

Brinker CJ, Dunphy DR (2006) Morphological control of surfactant-templated metal oxide films. Curr Opin Colloid Interface Sci 11:126–132

Choi BCK, Pak AWP (2006) Multidisciplinarity, interdisciplinarity and transdisciplinarity in health research, services, education and policy: 1. Definitions, objectives, and evidence of effectiveness. Clin Investig Med 29:351–364

Costacurta S, Malfatti L, Patelli A, Falcaro P, Amenitsch H, Marmiroli B, Grenci G, Piccinini M, Innocenzi P (2010) Deep X-ray lithography for direct patterning of PECVD films. Plasma Process Polym 7:459–465

Costacurta S, Falcaro P, Malfatti L, Marongiu D, Marmiroli B, Cacho-Nerin F, Amenitsch H, Kirkby N, Innocenzi P (2011) Shaping mesoporous films using dewetting on X-ray pre-patterned hydrophilic/hydrophobic layers and pinning effects at the pattern edge. Langmuir 27:3898–3905

Davis ME (2002) Ordered porous materials for emerging applications. Nature 417:813–821

del Campo A, Arzt E (2008) Fabrication approaches for generating complex micro- and nanopatterns on polymeric surfaces. Chem Rev 108:911–945

del Campo A, Greiner C (2007) SU-8: a photoresist for high-aspect-ratio and 3D submicron lithography. J Micromech Microeng 17:R81–R95

Doshi DA, Huesing NK, Lu M, Fan H, Lu Y, Simmons-Potter K, Potter BG, Hurd AJ, Brinker CJ (2000) Optically defined multifunctional patterning of photosensitive thin-film silica mesophases. Science 290:107–111

Eichelbaum M, Rademann K (2009) Plasmonic enhancement or energy transfer? on the luminescence of gold-, silver-, and lanthanide-doped silicate glasses and its potential for light-emitting devices. Adv Funct Mater 19:2045–2052

Eichelbaum M, Rademann K, Mueller R, Radtke M, Riesemeier H, Goerner W (2005) On the chemistry of gold in silicate glasses: studies on a nonthermally activated growth of gold nanoparticles. Angew Chem Int Ed 44:7905–7909

Eichelbaum M, Rademann K, Hoell A, Tatchev DM, Weigel W, Stoesser R, Pacchioni G (2008) Photoluminescence of atomic gold and silver particles in soda-lime silicate glasses. Nanotechnology 19:135701

Falcaro P, Innocenzi P (2011) X-rays to study, induce, and pattern structures in sol-gel materials. J Sol Gel Sci Technol 57:236–244

Falcaro P, Costacurta S, Malfatti L, Takahashi M, Kidchob T, Casula MF, Piccinini M, Marcelli A, Marmiroli B, Amenitsch H, Schiavuta P, Innocenzi P (2008) Fabrication of mesoporous functionalized arrays by integrating deep X-ray lithography with dip-pen writing. Adv Mater 20:1864–1869

Falcaro P, Malfatti L, Kidchob T, Giannini G, Falqui A, Casula MF, Amenitsch H, Marmiroli B, Grenci G, Innocenzi P (2009) Hierarchical porous silica films with ultralow refractive index. Chem Mater 21:2055–2061

Falcaro P, Hill AJ, Nairn KM, Jasieniak J, Mardel JI, Bastow TJ, Mayo SC, Gimona M, Gomez D, Whitfield HJ, Riccó R, Patelli A, Marmiroli B, Amenitsch H, Colson T, Villanova L, Buso D (2011) A new method to position and functionalize metal-organic framework crystals. Nature Commun 2:A237

Fan H, Lu Y, Stump A, Reed ST, Baer T, Schunk R, Perez-Luna V, Lopez GP, Brinker CJ (2000) Rapid prototyping of patterned functional nanostructures. Nature 405:56–60

Faustini M, Vayer M, Marmiroli B, Hillmyer M, Amenitsch H, Sinturel C, Grosso D (2010) Bottom-up approach toward titanosilicate mesoporous pillared planar nanochannels for nanofluidic applications. Chem Mater 22:5687–5694

Faustini M, Marmiroli B, Malfatti L, Louis B, Krins N, Falcaro P, Grenci G, Laberty-Robert C, Amenitsch H, Innocenzi P, Grosso D (2011) Direct nano-in-micropatterning of TiO_2 thin layers and TiO_2/Pt nanoelectrode arrays by deep X-ray lithography. J Mater Chem 21:3597–3603

Feigin LA, Svergun DI (1987) Structure analysis by small-angle X-Ray and neutron scattering. Plenum Press, New York and London

Goettert J, Moser HO, Pantenburg FJ, Saile V, Steininger R (2000) ANKA—a synchrotron light source for X-ray based micromachining. Microsyst Technol 6:113–116

Hozumi A, Cheng DF (2011) Facile micropatterning of mesoporous titania film by low-energy electron beam irradiation. Mater Chem Phys 129:464–470

Hozumi A, Kimura T (2008) Rapid micropatterning of mesoporous silica film by site-selective low-energy electron beam irradiation. Langmuir 24:11141–11146

Innocenzi P, Falcaro P, Schergna S, Maggini M, Menna E, Amenitsch H, Soler-Illia JAA, Grosso D, Sanchez C (2004) One-pot self-assembly of mesostructured silica films and membranes functionalised with fullerene derivatives. J Mater Chem 14:1838–1842

Innocenzi P, Kidchob T, Falcaro P, Takahashi M (2008) Patterning techniques for mesostructured films. Chem Mater 20:607–614

Lebeau B, Innocenzi P (2011) Hybrid materials for optics and photonics. Chem Soc Rev 40:886–906

Levine JR, Cohen B, Chung JW, Georgopoulos P (1989) Grazing-incidence small-angle X-ray scattering: new tool for studying thin film growth. J Appl Crystallogr 22:528–532

Liu Y, Cui T, Coane PJ, Vasile MJ, Goettert J (2003) High-aspect-ratio microstructures fabricated by X-ray lithography of polymethylsilsesquioxane-based spin-on glass thick films. Microsyst Technol 9:171–175

Loechel B, Goettert J, Desta YM (2007) Direct LIGA service for prototyping: status report. Microsyst Technol 13:327–334

Lu Y, Yang Y, Sellinger A, Lu M, Huang J, Fan H, Haddad R, Lopez G, Burns AR, Sasaki DY, Shelnutt J, Brinker CJ (2001) Self-assembly of mesoscopically ordered chromatic polydiacetylene/silica nanocomposites. Nature 410:913–917

Malfatti L, Marongiu D, Costacurta S, Falcaro P, Amenitsch H, Marmiroli B, Grenci G, Casula MF, Innocenzi P (2010) Writing self-assembled mesostructured films with in situ formation of gold nanoparticles. Chem Mater 22:2132–2137

Malfatti L, Falcaro P, Marmiroli B, Amenitsch H, Piccinini M, Falqui A, Innocenzi P (2011) Nanocomposite mesoporous ordered films for lab-on-chip intrinsic surface enhanced Raman scattering detection. Nanoscale 3:3760–3766

Marmiroli B, Grenci G, Cacho-Nerin F, Sartori B, Ferrari E, Laggner P, Businaro L, Amenitsch H (2009) Free jet micromixer to study fast chemical reactions by small-angle X-ray scattering. Lab Chip Miniat Chem Biol 9:2063–2069

Marmiroli B, Grenci G, Cacho-Nerin F, Sartori B, Laggner P, Businaro L, Amenitsch H (2010) Experimental set-up for time resolved small-angle X-ray scattering studies of nanoparticles

formation using a free-jet micromixer. Nucl Instrum Methods Phys Res Sect B Beam Interact Mater Atoms 268:329–333
Martinez-Manez R, Sancenon F, Biyikal M, Hecht M, Rurack K (2011a) Mimicking tricks from nature with sensory organic-inorganic hybrid materials. J Mater Chem 21:12588–12604
Martinez-Manez R, Sancenon F, Hecht M, Biyikal M, Rurack K (2011b) Nanoscopic optical sensors based on functional supramolecular hybrid materials. Anal Bioanalytical Chem 399:55–74
Melde BJ, Johnson BJ (2010) Mesoporous materials in sensing: morphology and functionality at the meso-interface. Anal Bioanalytical Chem 398:1565–1573
Nazmov V, Reznikova E, Mohr J (2011a) Investigation of the radiation-induced thermal flexure of an X-ray lithography mask during a tilted exposure. J Vac Sci Technol B Microelectron Nanometer Struct 29:0110071–0110077
Nazmov V, Reznikova E, Mohr J, Saile V, Vincze L, Vekemans B, Bohic S, Somogyi A (2011b) Parabolic crossed planar polymeric X-ray lenses. J Micromech Microeng 21:015020
Nie S, Emory SR (1997) Probing single molecules and single nanoparticles by surface-enhanced Raman scattering. Science 275:1102–1106
Otten A, Koster S, Struth B, Snigirev A, Pfohl T (2005) Microfluidics of soft matter investigated by small-angle X-ray scattering. J Synchrotron Radiat 12:745–750
Ozin GA, Cademartiri L (2009) Nanochemistry: what is next? Small 5:1240–1244
Panine P, Finet S, Weiss TM, Narayanan T (2006) Probing fast kinetics in complex fluids by combined rapid mixing and small-angle X-ray scattering. Adv Colloid Interface Sci 127:9–18
Perennes F, Vesselli E, Pantenburg FJ (2002) Deep X-ray lithography at ELETTRA using a central beam-stop to enhance adhesion. Microsyst Technol 8:330–334
Perennes F, Marmiroli B, Tormen M, Matteucci M, Di Fabrizio E (2006) Replication of deep X-ray lithography fabricated microstructures through casting of soft material. J Microlithogr Microfabr Microsyst 5:011007
Roder H, Maki K, Cheng H (2006) Early events in protein folding explored by rapid mixing methods. Chem Rev 106:1836–1861
Romanato F, Businaro L, Tormen M, Perennes F, Matteucci M, Marmiroli B, Balslev S, Di Fabrizio E (2006) Fabrication of 3D micro and nanostructures for MEMS and MOEMS: an approach based on combined lithographies. J Phys, Conf Ser 34:904–911
Saile V, Wallrabe U, Tabata O, Korvink JG (2009) Liga and its applications. Wiley-VCH Verlag GmbH & Co KGaA, Hoboken NJ
Scott BJ, Wirnsberger G, McGehee MD, Chmelka BF, Stucky GD (2001) Dye-doped mesostructured silica as a distributed feedback laser fabricated by soft lithography. Adv Mater 13:1231–1234
Sukhorukov GB, Volodkin DV, Guenther AM, Petrov AI, Shenoy DB, Moehwald H (2004) Porous calcium carbonate microparticles as templates for encapsulation of bioactive compounds. J Mater Chem 14:2073–2081
Tatchev D, Hoell A, Eichelbaum M, Rademann K (2011) X-ray-assisted formation of gold nanoparticles in soda lime silicate glass: suppressed Ostwald ripening. Phys Rev Lett 106:085702
Tormen M, Grenci G, Marmiroli B, Romanato F (2011) X-ray lithography: fundamentals and applications. In: Stefan Landis (ed) Nano lithography. ISTE Ltd. and John Wiley & Sons, Inc., London and Hoboken, pp 1–86
Vyawahare S, Griffiths AD, Merten CA (2010) Miniaturization and parallelization of biological and chemical assays in microfluidic devices. Chem Biol 17:1052–1065
Walcarius A (2008) Electroanalytical applications of microporous zeolites and mesoporous (organo)silicas: recent trends. Electroanalysis 20:711–738
Walcarius A, Collinson MM (2009) Analytical chemistry with silica sol-gels: traditional routes to new materials for chemical analysis. Rev Anal Chem 2:121–143
Walcarius A, Kuhn A (2008) Ordered porous thin films in electrochemical analysis. Trends Anal Chem 27:593–603
Walcarius A, Mercier L (2010) Mesoporous organosilica adsorbents: nanoengineered materials for removal of organic and inorganic pollutants. J Mater Chem 20:4478–4511
Wang C, Jones RL, Lin EK, Wu WL, Rice BJ, Choi KW, Thompson G, Weigand SJ, Keane DT (2007) Characterization of correlated line edge roughness of nanoscale line gratings using small-angle X-ray scattering. J Appl Phys 102:024901
Wu CW, Aoki T, Kuwabara M (2004) Electron-beam lithography assisted patterning of surfactant-templated mesoporous thin films. Nanotechnology 15:1886–1889
Zschech E, Wyon C, Murray CE, Schneider G (2011) Devices, materials, and processes for nanoelectronics: characterization with advanced X-ray techniques using lab-based and synchrotron radiation sources. Adv Eng Mater 13:811–836